Journal of Drug Delivery Science and Technology 62 (2021) 102348

Contents lists available at ScienceDirect

Journal of Drug Delivery Science and Technology

journal homepage: www.elsevier.com/locate/jddst

Research paper

Liposomes containing 3-arylamino-nor-β-lapachone derivative: Development, characterization, and in vitro evaluation of the cytotoxic activity

Luciana V. Rebouças [a], Fátima C.E. Oliveira [a], Daniel P. Pinheiro [a], Maria Francilene S. Silva [a], Vanessa Pinheiro G. Ferreira [b], Roberto Nicolete [b], Augusto C.A. Oliveira [a], Renata G. Almeida [c], Eufrânio N. da Silva Júnior [c], Marcia S. Rizzo [d], Marcília P. Costa [d,*], Guilherme Zocolo [e], Fábio O.S. Ribeiro [f], Durcilene A. da Silva [f], Claudia Pessoa [a]

[a] Laboratory of Experimental Oncology, Department of Physiology and Pharmacology, Federal University of Ceará, 60430-275, Fortaleza, CE, Brazil
[b] Fundação Oswaldo Cruz Ceará (FIOCRUZ-CE), 61760-000, Eusébio-CE, Brazil, Post-graduate Program Northeast Biotechnology Network (RENORBIO) Itaperi Campus 60, 714-903, Fortaleza, CE, Brazil
[c] Institute of Exact Sciences, Department of Chemistry, Federal University of Minas Gerais, 31275-013, Belo Horizonte, MG, Brazil
[d] Interdisciplinary Laboratory for Advanced Materials, Federal University of Piauí, 64049-550, Teresina, PI, Brazil
[e] Embrapa Tropical Agroindustry, 60511-110, Fortaleza, CE, Brazil
[f] Biodiversity and Biotechnology Research Center, Biotec, Federal University of Piauí, 64202-020, Parnaíba, PI, Brazil

ARTICLE INFO

Keywords:
Naphthoquinone
Drug delivery
Nanoencapsulation
Anticancer activity

ABSTRACT

This study aimed to encapsulate the novel synthetic naphthoquinone ENSJ39 in liposomes, characterize them, and evaluate their in vitro cytotoxic activity in different cancer cell lines. Liposomes were obtained by the dried-lipid film hydration method, and characterizations included thermogravimetric analysis, differential scanning calorimetry, dynamic light scattering technique, and atomic force microscopy. Simulation of storage conditions, in vitro cytotoxicity by MTT, Trypan blue exclusion assay, and evaluation of morphological changes in tumor cell lines were also analyzed. Liposomes containing ENSJ39 (LE39) exhibited an average size of 31 ± 5.81 nm, zeta potential of +53.5 mV, polydispersity index of 0.24, and high encapsulation efficiency (96.58 ± 0.09%). They were thermally stable up to 250 °C and able to preserve the mass loss of the free drug. After four months of storage, they maintained excellent physical-chemical characteristics. The encapsulated drug showed less cytotoxic activity than the free drug only in HCT-116 and SNB-19 cells and caused cytoplasmic vacuolization plus an increase in the number of non-viable HCT-116 cells. ENSJ39 encapsulation method was effective in obtaining stable liposomes that presented substantial cytotoxicity activity against tumor cell lines.

1. Introduction

Cancer is a worldwide public health problem, characterized by uncontrolled cell proliferation [1]. According to the World Health Organization (WHO), over 18 million new cancer cases were reported in 2018, and the most prevalent were lung (11.6%), breast (11.6%), colorectum (10.2%), and prostate (7.1%) [2]. International estimates from studies in more than 100 countries around the world indicate cancer as the first or second leading cause of premature death (in people aged 30–69). These studies predict 29 million cases by 2040, due to global aging and population growth [3]. In low- and middle-income countries, the incidence of cancer and death is generally even higher [4].

Despite the considerable arsenal of drugs already available for cancer treatment, in many cases, therapeutic success is not achieved due to failures in therapeutic schemes as a result of resistance, reduced patient survival, high rates of relapse, reduced tumor selectivity, low therapeutic efficacy, adverse effects, and unsustainable costs [5]. Thus, extensive research and investment are focused on developing increasingly potent and less toxic compounds.

Various studies have demonstrated the biological potential of naphthoquinones. This class of compounds presents microbicidal, trypanosomicidal, molluscicidal, anti-inflammatory, leishmanicidal,

* Corresponding author. Federal University of Piauí, College of Pharmacy, Health Sciences Center, Piauí, Teresina, Brazil, Ininga, 64049-550,
E-mail address: marciliapc@ufpi.edu.br (M.P. Costa).

https://doi.org/10.1016/j.jddst.2021.102348
Received 27 August 2020; Received in revised form 29 December 2020; Accepted 11 January 2021
Available online 19 January 2021
1773-2247/

virucidal, and antivenom properties [6–15]. The antitumor potential of quinoidal compounds is also widely known and well-studied [16–21].

The antitumor ability of naphthoquinones is generally determined by their structural framework, in particular their redox system consisting of carbonyl groups, which is an essential redox center capable of generating reactive oxygen species (ROS). The generation of ROS is intrinsically related to the antitumor properties of quinonoid compounds. The reduction process can be catalyzed biologically through one- or two-electron reducing enzymes. NADPH-cytochrome P450 reductase and NAD(P)H quinone oxidoreductase 1 (NQO1) are examples of enzymes that can act as redox agents [16,22]. The reduction processes are responsible for generating elevated amounts of ROS, resulting in the stimulation of oxidative stress and alkylation of cellular nucleophiles (including DNA, lipids, protein, and other biomolecules). These effects are described as mechanisms of cytotoxicity, leading to cell damage [23, 24].

A survey of publications in the last 20 years on PubMed and Web of Science databases, using the descriptors 'naphthoquinone and cancer', revealed a total of 3236 articles, indicating that the number of papers has quintupled since early 1999. The number of publications related to this chemical class demonstrates the growing interest in its pharmacology and mechanism of action in oncology.

Among naphthoquinones reported in literature, the compound 2,2-dimethyl-3-((2-methyl-4-nitrophenyl)amino)-2,3-dihydronaphtho(1,2-*b*)furan-4,5-dione (ENSJ39), a nor-β-lapachone derivative, demonstrated potent cytotoxic activity displaying IC_{50} values less than 2 μM against several cancer cell lines such as HL-60, MDA-MB-435, HCT-8, HCT-116, and SF-295 [16,19,25]. This compound induced apoptosis (mitochondrial pathway) and intracellular ROS generation in HL-60 cells, as well as DNA strand breaks in LNCap ($NQO1^-$) and DU-145 ($NQO1^+$) cells [20,26]. However, at the same time, ENSJ39 has poor solubility, which makes *in vivo* administration difficult, interfering with subsequent studies.

Moreover, previous studies with similar naphthoquinones have shown that certain compounds from this class are responsible for *in vivo* toxic effects, including hemolytic anemia and renal tubular necrosis in animals [27–31]. Solubility problems have also been reported [27,32, 33].

Drug delivery strategies to improve bioavailability and reduce toxicity have been applied to naphthoquinoidal compounds [34–38]. The incorporation of nanotechnology has proved quite promising compared to traditional medicine. This approach allows the development of encapsulated drugs with reduced off-target toxicity, increasing the concentration of the drug in a particular target, improving the therapeutic efficacy, and also addressing problems related to the physicochemical properties of the non-encapsulated substance, such as solubility and stability [39,40].

Liposomes can be used to deliver low molecular weight drugs, large proteins, and even therapeutic nucleic acid sequences. Constituted by a bilayer lipid vesicle between 50 nm and 5 μm in size, the similarity of liposomes to biological membranes endows them with particular properties, such as biocompatibility and biodegradability. Therefore, liposomes are highly versatile nanostructures for encapsulation and delivery of bioactive agents in nanomedicine applications [41–44].

Due to the importance of naphthoquinones in the progress of pharmacological studies focusing on cancer treatment and knowing the advantages of using liposomes, the present study aimed to evaluate the in vitro physical-chemical and biological characteristics of liposomes containing the new synthetic naphthoquinone ENSJ39.

2. Material and METHODS

2.1. Material

The chemical compound 2,2-dimethyl-3-((2-methyl-4-nitrophenyl) amino)-2,3- dihydronaphtho(1,2-b)furan-4,5-dione, named by our research group as ENSJ39, was synthesized from lapachol as previously described in the literature [16,19] (Fig. 1). Soybean phosphatidylcholine (PC), cholesterol (CH), stearylamine (SA), trehalose, and Trypan blue dye were purchased from Sigma-Aldrich (Missouri, USA). Acetonitrile, chloroform, methanol, and dimethyl sulfoxide (DMSO) were obtained from Merck (Darmstadt, Germany). All chemicals were of analytical grade. Fetal bovine serum and Dulbecco's modified eagle medium (DMEM) were purchased from Cultilab (São Paulo, Brazil). RPMI 1640 medium, trypsin-EDTA, penicillin, and streptomycin were purchased from GIBCO (California, USA). Doxorubicin (Doxolem) was purchased from Zodiac Produtos Farmacêuticos S/A (Brazil). The Quick Panoptic kit was obtained from Laborclin (Paraná, Brazil).

2.2. Development of liposomal formulations

ENSJ39 liposomes (LE39) were prepared by the dried-lipid film hydration method followed by sonication, as previously reported [45]. Briefly, PC, CH, and SA (7:2:1 M ratio) were dissolved in a mixture of chloroform and methanol (3:1 v/v) under magnetic agitation. ENSJ39 (1:28.48 drug/lipid molar ratio) was then added to the organic lipidic phase. Unloaded liposome (LBR) was synthesized in the same way without the drug (ENSJ39).

A dried-lipid film was obtained through evaporation of organic solvents under reduced pressure at 38 ± 1 °C for 30 min, rotation of 80 rpm, using an IKA RV10 Rotary Evaporator (Wilmington, USA). The resulting lipid layer was hydrated with 10 mL of phosphate buffer solution (PBS) (pH 7.4) with or without trehalose (0.1, 5, and 10%), to obtain multilamellar liposomes in suspension (0.6 mg/mL of ENSJ39). Then, small unilamellar vesicles were obtained by sonication using a Qsonic probe (Newtown, USA), operating in pulsate mode with a potency of 125 W and a frequency of 20 kHz for 300 s (5 s on/2 s off). Finally, LE39 and LBR were frozen overnight and freeze-dried (MicroModulyo Freeze Dryer; Thermo, USA) in 200 bars for 24 h and stored at 8 °C. Both formulations were also stored at 8 °C to be monitored after 24 h of preparation.

2.3. Measurement of particle characteristics

The particle size, size distribution, and zeta potential of LE39 and LBR diluted (1:100 w/v) were determined by Malvern Zetasizer Nano-ZS90 (Worcestershire, UK) at 25 °C scattering angle of 90°. Liposome samples were diluted with ultrapure water and sonicated before measurement, as required, for a satisfactory particle count. The distribution and the mean diameter of particles were evaluated as well as their standard deviation and polydispersity index (PDI). Data were obtained by averaging ten measurements.

The number of particles per mL of lyophilized liposomes (LE39 and LBR) were investigated in NanoSight NS500 equipment (Marven, UK). The LE39 and LBR liposome suspensions, previously diluted 1: 40,000 in purified water, were injected into the visualization camera. Three different batches of each sample were used, and the results were expressed as average.

Particle morphological analysis was performed using an Atomic Force Microscopy (AFM) as previously described [46]. Briefly, 10 μL of diluted samples (1:10 v/v) was sonicated for 15 min, spread onto freshly cleaned mica disks, and dried for around 15 min at 36 °C. LE39 and LBR were analyzed using the AFM Workshop TT-AFM microscopy (California, USA). The images were taken in tapping mode using a silicon cantilever (TAP 300-G10, TED PELLA) with a resonance frequency of approximately 238 kHz. The images were processed using Gwyddion 2.45 software.

Thermal analysis of ENSJ39 and lyophilized liposomes (LE39 and LBR) were investigated by Thermogravimetric Analysis (TGA) and Differential Scanning Calorimetry (DSC) performed, respectively, in Perkin Elmer STA 6000 (Massachusetts, USA) and Shimadzu DSC-60 (Kyoto, Japan). Measurements were performed at a temperature range from 25

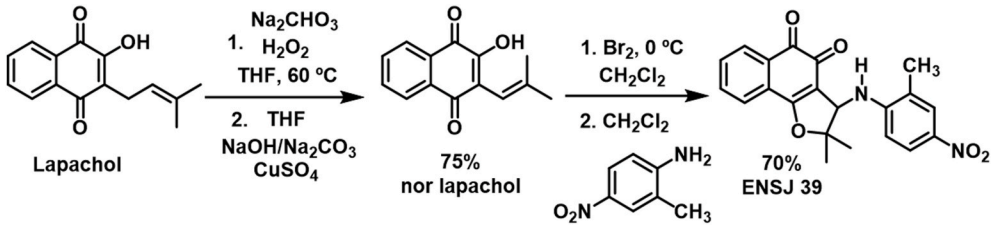

Fig. 1. Synthetic route to obtain naphthoquinone ENSJ39 [19].

to 400 °C (TGA) at a heating rate of 10 °C/min under nitrogen flow (50 mL/min) by using a closed aluminum pan, in which approximately 10 mg of the sample was placed. Thermograms obtained by DSC of lyophilized liposomes and pure drug were performed at a temperature range from 25 to 240 °C at a heating rate of 10 °C/min under a dynamic nitrogen atmosphere using a closed aluminum pan, in which approximately 10 mg of the sample was placed.

2.4. Encapsulation efficiency

Drug content was determined using the Genesys 10S UV–Vis spectrophotometer (Thermo, Massachusetts, USA) at 256 nm. The calibration curve of ENSJ39 in acetonitrile was accomplished using six standard solutions in the range of 2–50 μg/mL prepared from a stock solution (0.2 mg/mL). Then, samples of LE39 and LBR were quantified as a total fraction and purified liposomal fraction.

To determine the total drug content in the formulations, liposomes were diluted (1:10 w/v) in acetonitrile, sonicated for 15 min, filtered through a PTFE membrane (0.22 μm), and analyzed by spectrophotometry. To separate the non-encapsulated drug, LE39 was preliminarily filtered through an Ultrafree® centrifugal filter (Millipore, USA). The free drug in the supernatant was measured after centrifugation of the sample at 5000 rpm for 2 h. Then, it was diluted (1:10 w/v) in acetonitrile, sonicated for 15 min, filtered through a PTFE membrane (0.22 μm), and analyzed by spectrophotometry. Assays were performed in triplicate.

The absorbance value of LE39 was subtracted from the absorbance value of LBR in each procedure and then used in the equation of the calibration curve to obtain concentrations of drugs in total and purified liposomal fraction. Next, the encapsulation efficiency (EE) was calculated according to Equation (1).

$$EE\ (\%) = \frac{\text{concentration of drug in purified liposomal fraction } (\mu g/mL)}{\text{concentration of drug in total fraction } (\mu g/mL)} \times 100 \quad (1)$$

2.5. Evaluation of stability

Liposomes stability was evaluated using long-term stability testing, as described by Cavalcanti [38], with modifications. Particle size, zeta potential, and polydispersity index (PDI) of the diluted liposomal formulations (1:100 w/v) were monitored after 24 h of preparation and during storage, at predetermined time intervals (1–4 months) at room temperature (25 °C) and under refrigeration (8 °C). For long-term stability evaluation, LE39 and LBR were diluted in purified water at 1/100 (w/v). Measurements were performed using a Malvern Zetasizer Nano-ZS90 (Worcestershire, UK).

2.6. Cytotoxicity assay

The cytotoxicity of ENSJ39 and liposomes were evaluated against HCT-116 (7×10^4 cells/well), SNB-19 (1×10^5 cell/well), HL-60 (3×10^5 cells/well), PC-3 (1×10^5 cell/well), B16F10 (7×10^4 cells/well), and normal murine fibroblast L929 (7×10^4 cells/well) cells by the colorimetric MTT (3-(4,5-dimethylthiazol-2-yl)-2,5-diphenyl tetrazolium bromide)) assay, as described by Mosmann [47], with modifications. Cell lines were maintained in flasks containing RPMI 1640 or DMEM medium supplemented with 10% fetal bovine serum, 100 U/mL penicillin, and 100 μg/mL streptomycin at 37 °C and 5% CO_2 atmosphere.

ENSJ39 and liposomes were diluted in culture medium in a serial dilution of 0.03–3.78 μg/mL, added to the cells seeded in 96-well plates and incubated for 72 h, at the same conditions described above. Doxorubicin (0.04–2.72 μg/mL) was used as a positive control. After 72 h incubation, 100 μL of MTT solution (0.5 mg/mL) was added to each well, and cells were incubated for 3 h. Then, the supernatant was removed, 100 μL of DMSO was added to solubilize the formazan crystals, and the absorbance was measured using a microplate spectrophotometer (DTX800 Multimode Detector, Beckman Coulter, California, USA) at 595 nm. The absorbances obtained were used to calculate the IC_{50} values by nonlinear regression employing appropriate statistical software. Statistical significance was calculated by Analysis of Variance (ANOVA) followed by Tukey's test, with a significance level of $p < 0.05$. All treatments were performed in triplicate in at least three independent experiments.

2.7. Trypan blue exclusion assay

HCT-116 tumor cells were chosen for this assay and the morphological analysis described below (topic 2.8), because this cell line has been used in previous studies carried out by our group to elucidate the mechanisms of action for ENSJ39 (Unpublished data) [25].

Trypan blue exclusion assay was performed as described by Strober [48], with modifications. This assay is based on the principle that living cells possess intact cell membranes that exclude certain dyes, such as Trypan blue, whereas dead cells do not.

HCT-116 cells were seeded in six-well plates at a seeding density of 5×10^4 cells/well and treated with ENSJ39 and LE39 (considering the encapsulation efficiency) at concentrations of 2.32 μg/mL and 3.48 μg/mL. Untreated cells represented negative control, and doxorubicin 1 μg/mL was used as a positive control. After 72 h of treatment, cells were harvested, centrifuged for 5 min at 1500 rpm, and resuspended in 1 mL of PBS. Then, 90 μL of the cell suspension was mixed with 10 μL of 0.4% Trypan blue dye for counting viable and non-viable cells in a Neubauer chamber under an optical microscope (Nikon Eclipse E100, Tokyo, Japan). Assays were performed in triplicate in at least three independent experiments.

Data were calculated from mean ± standard deviation (SD) and compared by Analysis of Variance (ANOVA) followed by Tukey's test, with a significance level of $p < 0.05$, using appropriate statistical software.

2.8. Morphological analysis of HCT-116 cells

The morphological analysis allowed evaluation of possible modifications related to cell death patterns after treatment with the tested samples. HCT-116 cells were seeded in 24-well plates, with circular coverslips at the bottom of each well, at a seeding density of 5×10^4 cells/well. The next day, cells were treated with ENSJ39 and LE39

(considering the encapsulation efficiency) at concentrations of 2.32 μg/mL and 3.48 μg/mL. Untreated cells represented negative control.

After 72 h, the coverslips were removed and stained with the Quick Panoptic kit, which contains 0.1% triarylmethane solution 1 (fixative), 0.1% xanthene solution 2 (cytoplasm dye), and 0.1% thiazine solution 3 (nucleus dye). After staining, cells were evaluated under an optical microscope (Nikon Eclipse E200, Tokyo, Japan) coupled to a camera.

3. Results and DISCUSSION

3.1. Characterization of LE39 and LBR

Liposomes prepared by the dried-lipid film hydration method obtained satisfactory results, such as small particle size, high zeta potential values, and low PDI values. LE39 exhibits an average diameter of 31 ± 5.81 nm, the zeta potential of +53.5 ± 1.41 mV, and PDI of 0.24 ± 0.01. Similar results were obtained for LBR liposomes: particle size of 33 ± 7.71 nm, the zeta potential of +58.3 ± 2.04, and PDI of 0.23 ± 0.02. LE39 and LBR liposome suspensions contained around 1380 and 579 billion particles/mL, respectively.

The particle size obtained for liposomes in the present study is within the definition of lipid nanoparticles [43,49]. Zeta potential values were close to +60 mV, which are considered optimal and indicate colloidal stability due to strong electrostatic repulsions between particles and decreased tendency to aggregate [50,51]. PDI values were less than 0.25, indicating a very narrow distribution, resulting in a homogeneous system [49,51], which was confirmed by the particle size distribution of LE39 (Fig. 2a).

Processing techniques have been reported in the literature which ensure that those characteristics are maintained and the half-life of the formulation increases. The use of freeze-drying is an alternative procedure, as the dry state has greater stability and allows the formulation to be reconstituted with a vehicle at the time of administration [53]. During this process, cryoprotectants are commonly employed to avoid ice crystals that could damage the liposomes. In lipid nanoformulations, the use of trehalose, glucose, sucrose, or mannitol can form a protective glassy matrix in the nanoparticles [43,54,55].

We evaluated the particle size, zeta potential, and PDI in freeze-dried formulations. Trehalose at concentrations of 5% and 10% was effective in maintaining the fundamental characteristics of LE39 (Fig. 2), allowing the preservation and stability of the nanostructures. Trehalose is an excellent cryoprotectant for the lyophilization process of liposomal nanosystems [43,56], and its use has already been reported in the literature, with concentrations ranging from 0.1 to 10% [38,57].

Concerning the morphological aspects, AFM images of the liposomes showed regular spherical shape, smooth surface, and absence of agglomerates for both ENSJ39-loaded and unloaded liposomes (Fig. 3). The liposomes were flattened and slightly deformed, probably due to the adsorption on the mica surface, which can interfere with the average diameter of particles [58].

The 2D phase image in Fig. 3 illustrates two regions of the liposome: a central nucleus (yellow arrow) surrounded by a membrane (white arrow). This confirmed that the formulated nanoparticles had appropriate liposomal morphological characteristics compatible with a unilamellar vesicle structure [59].

The lipid membrane was thicker in LE39 than in LBR (Fig. 3a and b, white arrow), suggesting that ENSJ39, a lipophilic compound, was incorporated within the liposomal phospholipid bilayer. This may contribute to greater stability and compacting of liposomes. A similar phenomenon occurs when cholesterol is used in the preparation of liposomes. Voluminous steroid rings of cholesterol are interspersed among the phospholipid bilayer and provide rigidity and greater stability to the nanoparticle [60,61].

In the thermal analysis of ENSJ39 and liposomes, the TGA curve (Fig. 4a) indicated that LE39 and LBR are thermally stable up to 228 °C, while ENSJ39 degrades at 25 °C. This degradation was preserved in the liposomes. The mass loss for LE39 was lower than that for ENSJ39 (free drug) up to 328 °C. Above this temperature, the degradation of the free drug remained stable. Rapamycin and paclitaxel were also protected from degradation when encapsulated in liposomes [61]. Likewise, the thermogravimetric evaluation of liposomes containing β-lapachone showed that the encapsulation system prevented degradation as occurred in free drug [38].

The DSC thermogram (Fig. 4b) displays endothermic peaks compatible with the melting of the material (crystalline to amorphous state) in ENSJ39, LE39, and LBR samples at 112 °C, 164 °C, and 177 °C, respectively. The melting peaks of LE39 and LBR showed similar aspects. The first one suffered a slight broadening at its base and presented intermediate melting temperature compared to free drug and unloaded liposomes.

A double melting peak in ENSJ39 may indicate polymorphism, which means the presence of different crystalline morphologies (Fig. 4b). The disappearance of this peak in the DSC thermogram of LE39 may denote the absence of the drug crystalline state, suggesting that the drug was entrapped and molecularly dispersed in an amorphous state into the liposome [35,62,63]. That may have contributed to improving the solubility of the compound, as amorphous drugs are more soluble than crystalline ones, resulting in higher bioavailability [62,64]. The freeze-dried sample of LE39 was easily dispersed in an aqueous vehicle as opposed to the free drug, which requires an organic solvent like DMSO.

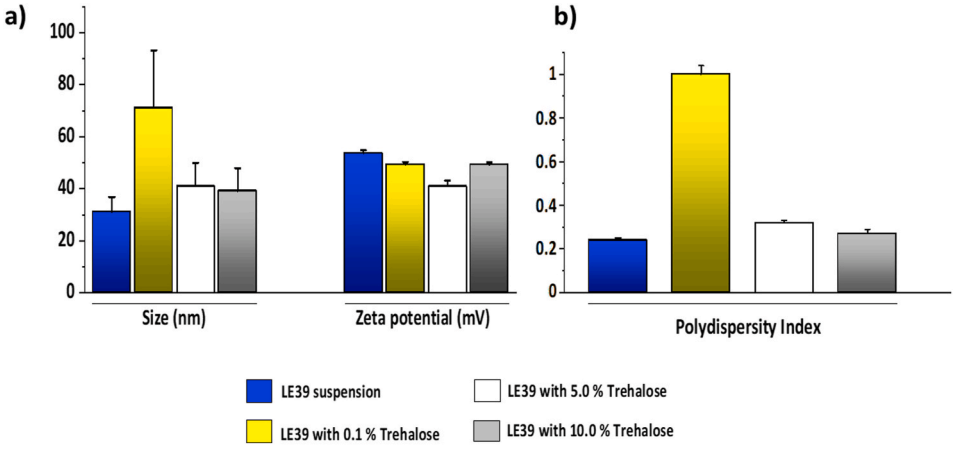

Fig. 2. Characterization of LE39 liposomes. Values of particle size and zeta potential (a), and polydispersity index (PDI) (b) of the LE39 suspension and freeze-dried with three different trehalose concentrations (0.1%, 5%, and 10%).

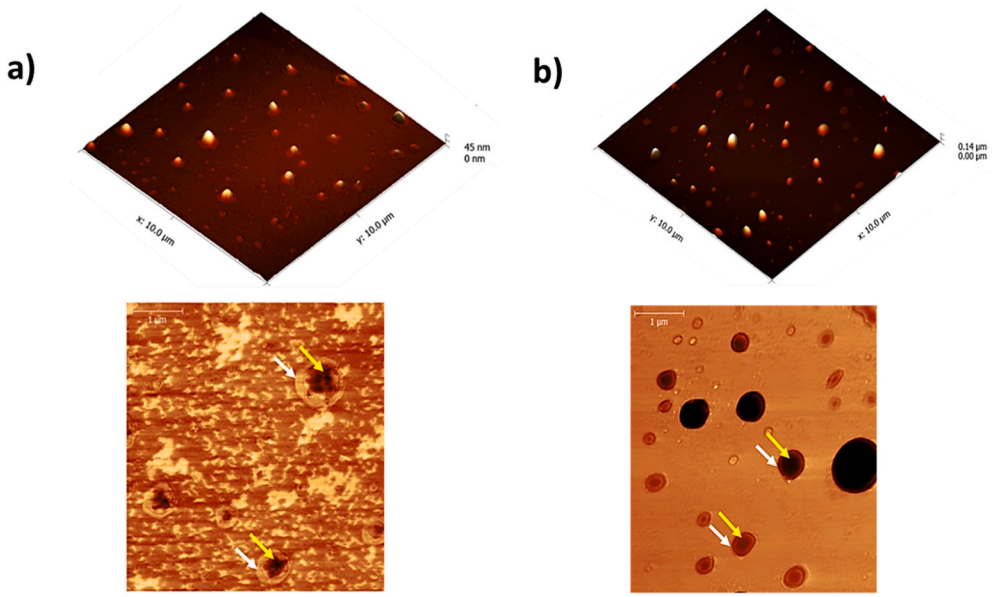

Fig. 3. AFM images of liposomes containing ENSJ39 (LE39) (a) and unloaded liposome (LBR) (b). White arrows indicate the membrane of phospholipids, and yellow arrows indicate the central nucleus. (For interpretation of the references to color in this figure legend, the reader is referred to the Web version of this article.)

3.2. Encapsulation efficiency

The data obtained from the analytical calibration curve of ENSJ39 yielded the following linear regression equation ($r^2 = 0.9984$): absorbance = 0.0308 x ENSJ39 concentration (μg/mL) + 0.0161. The total drug content in the liposomes was 82.3% (±0.04). Following this equation, concentrations of the drug in purified fraction and total liposomal fraction were calculated and applied to Equation (1), resulting in 96.58% (±0.09) of encapsulation efficiency.

This method of determining the encapsulation efficiency by UV/visible spectrophotometry has also been applied in other studies involving different liposomal nanoformulations [57,65], including liposomes containing naphthoquinones [38,66]. The remarkable encapsulation ratio of ENSJ39 is in agreement with other efficiency values of β-lapachone into liposomes, using the same lipid film method and similar preparation conditions as LE39: 97.09% [38] and 97.4% [66]. The extent of encapsulation efficiency in liposomal systems is generally higher for non-polar drugs than for polar drugs [59], which corroborates the rate obtained for LE39, as ENSJ39 is a highly non-polar compound.

Naphthoquinone drugs appear to have better rates when encapsulated in liposomal nanosystems. Previous data showed an encapsulation efficiency of 41.9% for β-lapachone in PLA-PEG micelles [67], and its encapsulation in PLGA-microcapsules had a trapping rate of 19.36% [35].

3.3. Stability evaluation of liposomes

ENSJ39 liposomes (LE39) stored at room temperature (25 °C) and under refrigeration (8 °C) did not exhibit drug precipitation and lipid flocculation when evaluated 24 h after preparation (Fig. 5). During the evaluation period of four months, a small precipitate of easy resuspension was observed after one month of storage in both conditions (Fig. 5).

After four months of storage, zeta potential values decreased (Fig. 6); however, at 8 °C, they remained within a range considered stable (˃ ± 30 mV) [52]. Furthermore, particle size, size distribution, and PDI values of LE39 stored at 8 °C were similar to those in the initial condition (Fig. 6), suggesting this is a better storage option than 25 °C.

These results are in agreement with a similar study of β-lapachone encapsulated in liposomes by the lipid film method using the same drug: lipid molar ratio and PC:CH:SA molar ratio as here. β-lapachone liposomes were resistant to accelerated stability tests and maintained their initial properties even after 60 days, in suspension form, and up to 1 year, in the freeze-dried form [38].

3.4. In vitro cytotoxicity

The IC_{50} values, obtained after 72 h treatment, for ENSJ39 and LE39 are presented in Table 1, along with data obtained for doxorubicin (positive control).

The IC_{50} values for ENSJ39 did not undergo significant changes between tumor cell lines, exhibiting cytotoxic activity for all of them, with higher cytotoxicity for HL-60 cells. Previous studies for ENSJ39 and other arylamine analogs revealed potent cytotoxic activity, with some compounds displaying IC50 values less than 1 μM against the tumor cell lines HL-60, MDA-MB-435, HCT-8, SF-295, PC-3, and B-16 [16,19,20,26].

A previous study of the mechanisms of action for ENSJ39 [25] suggested its bioactivation by the NQO1 enzyme (Unpublished data). As observed in Table 1, ENSJ39 exhibited potent activity in HL-60 tumor cells, even though this cell line is reported to have reduced expression of NQO1 [68]. This result corroborates with previous data, in which arylamino-nor-β-lapachone analogs had considerable activity against the same leukemia cell line, also similar to the effect observed with the precursor molecule (nor-β-lapachone) [20,26]; thus suggesting that ENSJ39 bioactivation can be induced by other reductases, in addition to NQO1. No bioreductive antitumor agent is activated by a single reductive enzyme [69]. Moreover, some experiments using dicoumarol (NQO1 inhibitor) and naphthoquinone drugs have shown that despite the protection of tumor cells overexpressing NQO1, no cell lines have exhibited significantly reduced expression of this enzyme, as HL-60 cells [70,71]. In any case, even though studies on the cytotoxicity of ENSJ39 have been conducted, this compound is new; therefore, its exact mechanism is still being unraveled.

There was a statistical difference in cytotoxicity between LE39 and ENSJ39 for HCT-116 and SNB-19 cells (Fig. 7). The encapsulated drug showed less cytotoxic activity than the unencapsulated one on those tumor cell lines.

In any case, according to a cytotoxic activity classification reported by Pérez-Sacau et al. [72] and Costa et al. [35], both ENSJ39 and LE39

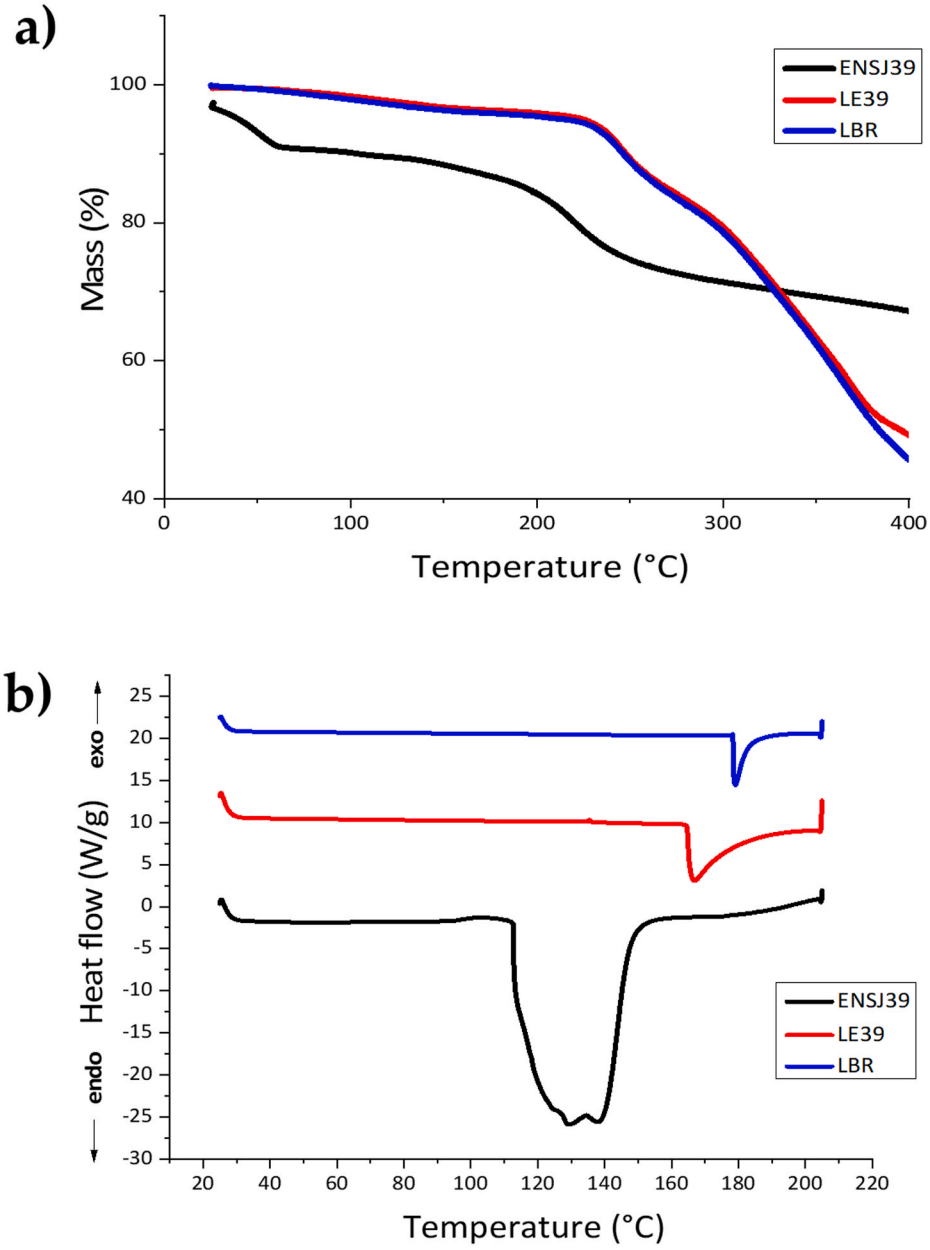

Fig. 4. Thermogravimetric Analysis (TGA) (a) and Differential Scanning Calorimetry (DSC) (b), ENSJ39 drug, liposomes containing ENSJ39 (LE39), and unloaded liposome (LBR) curves.

were highly active (IC_{50} < 1 μg/mL) to HL-60 cells and moderately active (1 μg/mL < IC_{50} < 10 μg/mL) to the other tested cell lines. The cytotoxicity was also evaluated in empty liposomes (LBR), and it did not demonstrate significative proliferative inhibition (data not shown).

In agreement with our results, other comparative studies evaluating cytotoxicity of free drugs and their encapsulated form showed differences in toxicity. The evaluation of free and liposome-encapsulated doxorubicin showed that cytotoxicity and uptake of the free drug were higher than in the nanoformulation [73,74]. Stealth liposomes of isoniazid and rifampicin also had less cytotoxicity than free drugs, even though both systems had the same cellular uptake [75].

In drug delivery systems, such as liposomes, less cytotoxicity can occur due to slower and more controlled release of the drug from liposomes compared to free drug, considering the same incubation time [34,73,74,76]. Furthermore, liposomes can interact with target cells in different ways depending on their lipid composition, steric stabilization, particle size, surface charge, and other aspects. Those parameters generate changes in the absorption patterns of the encapsulated drug and, consequently, influence the bioavailability and the magnitude of its cytotoxic effects on cells [57,77].

Liposomes have benefits related to a passive delivery in the tumor environment, which ensures that a higher concentration of drugs reaches the focus of action and with a longer release time [41–43]. Moreover, although a free drug has effective in vitro cellular activity, at *in vivo* level, there is no guarantee that large concentrations of the drug will be able to reach the tumor site. Free doxorubicin, for example, which has suitable in vitro cellular uptake, has difficulty reaching the tumor site *in vivo*, as it disappears by rapid opsonization and is absorbed by the reticular endothelial system of the liver and spleen [73].

The ENSJ39 and LE39 were also analyzed by the Trypan Blue exclusion assay in HCT-116 cells. Both caused a reduction in the number of viable cells at 2.32 and 3.48 μg/mL, similar to the positive control (doxorubicin) (Fig. 8). When evaluating the number of non-viable cells, significant differences were observed in free and encapsulated ENSJ39

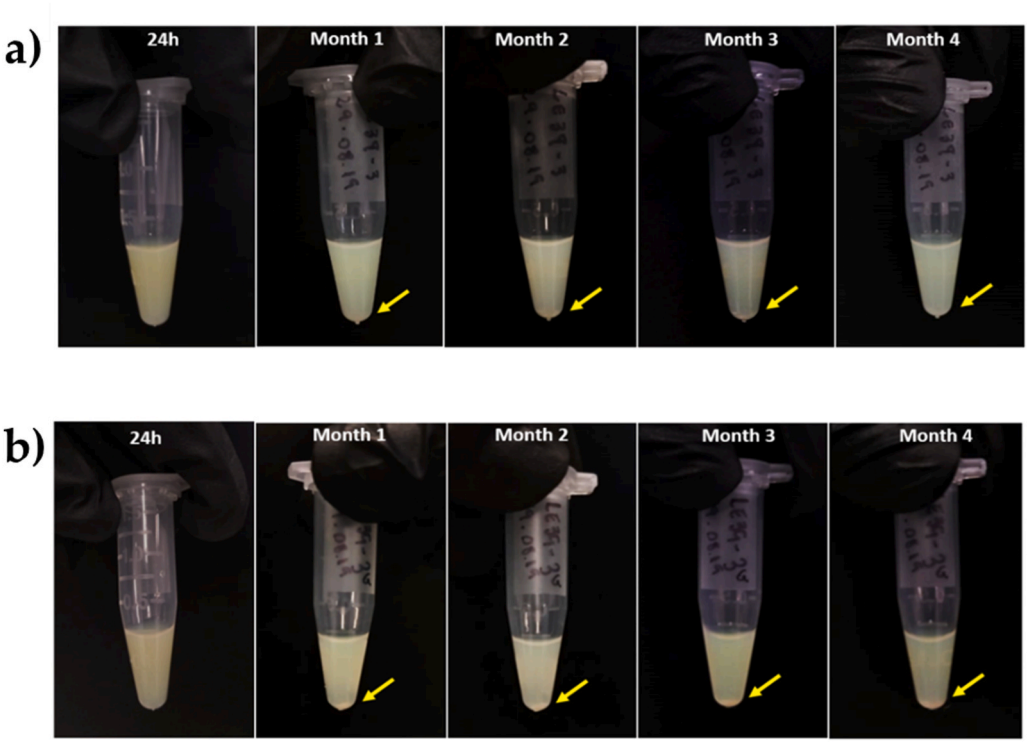

Fig. 5. LE39 subjected to stability evaluation at 25 °C (a) and 8 °C (b) for four months. Yellow arrows indicate precipitation. (For interpretation of the references to color in this figure legend, the reader is referred to the Web version of this article.)

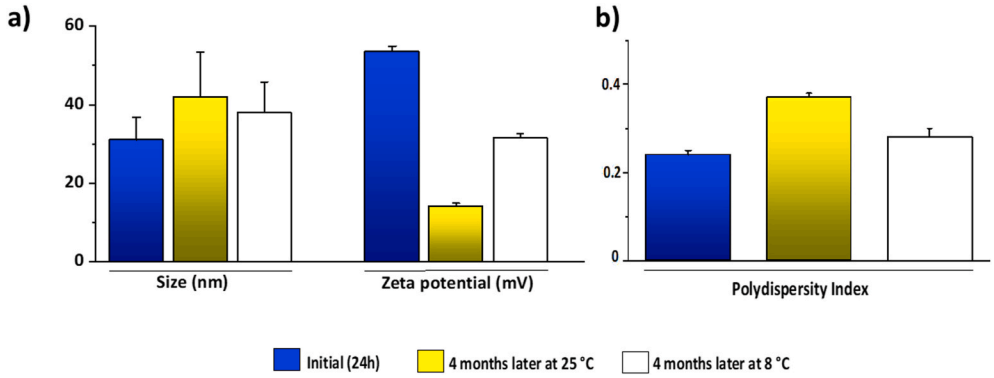

Fig. 6. Stability evaluation of LE39 liposomes. Evaluation of particle size, zeta potential (a), and PDI (b) of LE39 suspension after 24 h of preparation, four months later at 25 °C and 8 °C.

Table 1
Cytotoxic activity of ENSJ39, LE39 and Doxorubicin (DOX), as a positive control, evaluated by the MTT assay after 72 h of exposure for different cell lines.

Samples	IC_{50} (μg/mL) (CI 95%)[a]					
	HCT-116	PC-3	SNB-19	HL-60	B16F10	L929
ENSJ39	1.16 (1.08–1.25)	1.33 (1.19–1.48)	1.61 (1.40–1.85)	0.23 (0.20–0.27)	1.59 (1.52–1.65)	2.12 (1.92–2.34)
LE39	4.46 (3.41–5.83)	1.53 (1.14–2.05)	3.98 (3.50–4.52)	0.58 (0.53–0.64)	1.68 (1.11–3.31)	2.53 (2.28–2.80)
DOX	0.11 (0.09–0.16)	0.41 (0.32–0.51)	1.20 (1.03–1.39)	0.02 (0.01–0.02)	0.73 (0.61–0.88)	0.93 (0.86–1.02)

[a] IC_{50} values with 95% confidence intervals (CI) were obtained by non-linear regression from at least three independent experiments.

compared to controls. However, no significant differences were observed between concentrations.

The results obtained in the Trypan Blue assay and the MTT test were in agreement for the morphological disorders caused in HCT-116 cells after treatment with ENJ39 and LE39 for 72 h, in both tested concentrations (Fig. 9). While the negative control exhibited intact cells with well-defined cytoplasm and nucleus, ENSJ39 caused a notable decrease in the number of cells per field, intense cytoplasmic loss, membrane integrity loss (black arrows), reduction of cell volume, and nuclear pyknosis (white arrows) (Fig. 9). The cellular damage suggests an apoptotic process induced by ENSJ39, described by Pinheiro [25] and Cavalcanti [26] as reduced cell viability and increased number of cells with apoptotic characteristics (reduced cell volume, peripheral chromatin condensation, and apoptotic bodies) associated with reduced

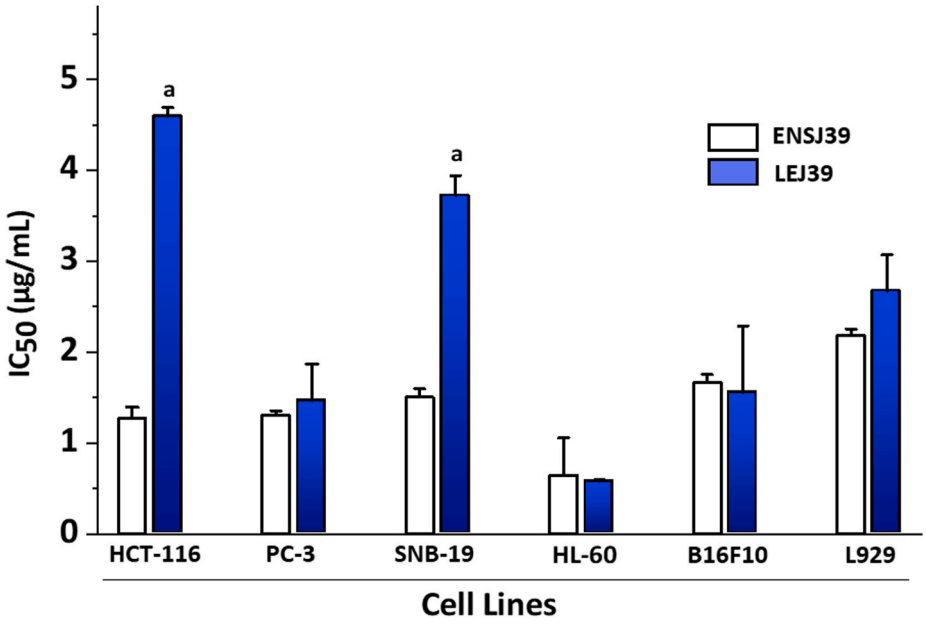

Fig. 7. IC_{50} values for free and encapsulated ENSJ39 (LE39) after 72 h treatment in different cell lines. Data are presented as mean ± SD from three independent experiments performed in triplicate. a = $p < 0.05$ compared to ENSJ39 treatment by ANOVA followed by Tukey's test.

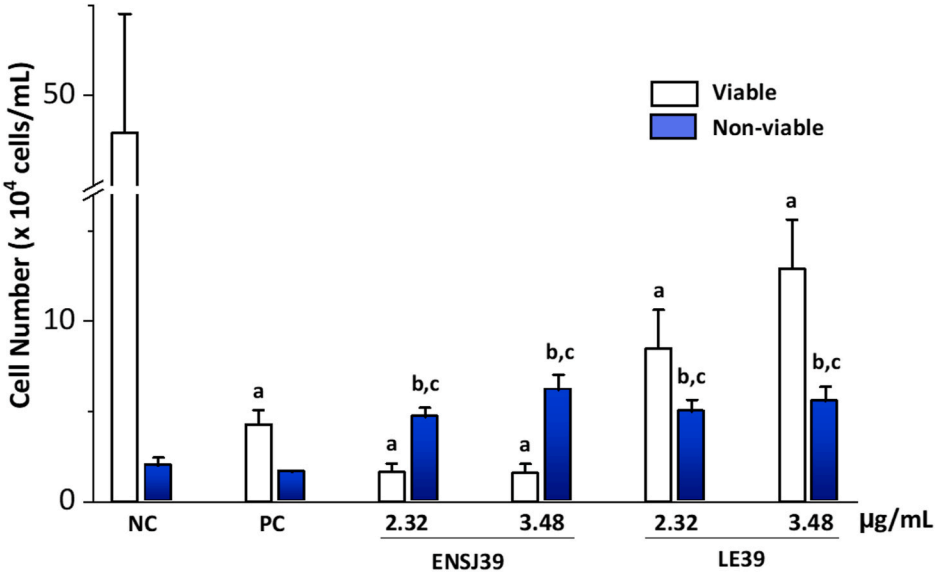

Fig. 8. Effect of ENSJ39 and LE39 on the viability of HCT-116 cells determined by the Trypan Blue exclusion assay after 72 h of treatment. Data are presented as mean ± SD from three independent experiments performed in triplicate. a = $p < 0.05$ compared to viable cells in the negative control; b = $p < 0.05$ compared to non-viable cells in the negative control; c = $p < 0.05$ compared to non-viable cells in the positive control by ANOVA followed by Tukey's test. (For interpretation of the references to color in this figure legend, the reader is referred to the Web version of this article.)

membrane integrity.

HCT-116 cells treated with LE39 displayed cell swelling and intense cytoplasmic vacuolization (red arrows), probably indicating cellular uptake of the liposomes. Mitotic events were found after LE39 treatment and negative control (green arrows), but not for the free drug. Cellular damage caused by the tested compounds was more intense at the highest concentration (3.48 µg/mL).

4. Conclusion

In this study, ENSJ39 liposomes (LE39) were developed using the dried-lipid film hydration method. LE39 formulation was characterized as a homogeneous system, stable after a four-month storage period, due to the high zeta potential values obtained. Thermal analysis, including DSC and TGA, indicated the successful coating of liposomes with ENSJ39 in an amorphous state, and the nanosystem was able to protect the drug from degradation. LE39 formulation was capable of encapsulating above 80% of ENSJ39 and can be quickly dispersed in an aqueous vehicle, unlike the free drug, improving the solubility of ENSJ39. *In vitro* cytotoxicity studies indicated that the free drug had higher activity in HCT-116 and SNB-19 cells, but ENSJ39 and LE39 had similar cytotoxic activity against other tumor cell lines exhibiting the most potent activity in HL-60 tumor cells. Morphological features compatible with an apoptotic cell death process were determined by optical microscopy. Therefore, those results support that ENSJ39 liposomes are viable and have a potential application in future *in vivo* studies, such as xenograft tumor models. However, only *in vivo* studies can prove the potential of these liposomes as a promising drug delivery system for antitumor therapy.

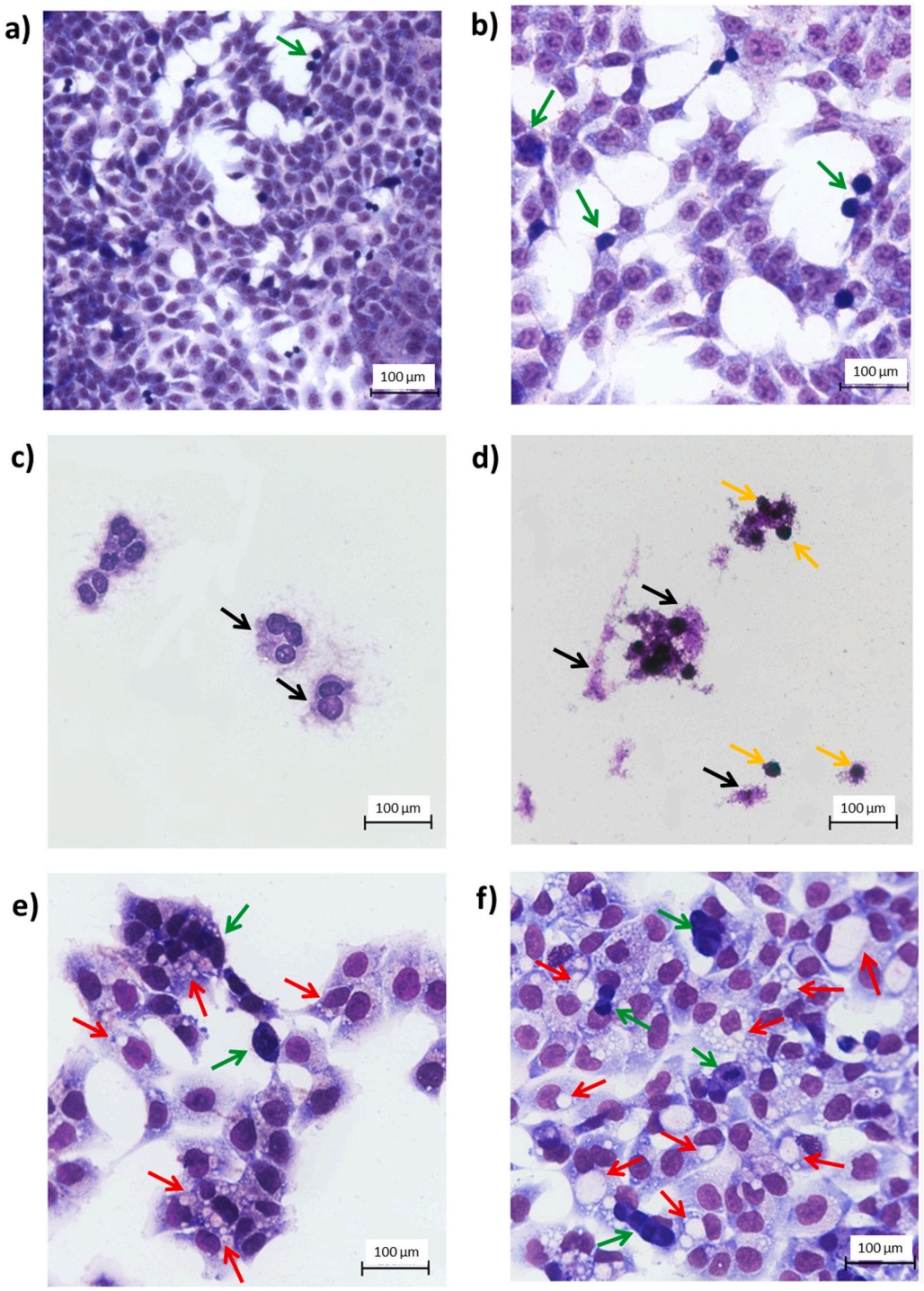

Fig. 9. Morphological analysis of HCT-116 cells after 72 h of treatment with different concentrations of ENSJ39 and LE39. (a) The negative control received no treatment; (b) ENSJ39 2.32 µg/mL; (c) ENSJ39 3.48 µg/mL; (d), LE39 2.32 µg/mL (e); and LE39 3.48 µg/mL. Green arrows indicate mitotic events, black arrows indicate cytoplasmic loss, yellow arrows indicate nuclear pyknosis, and red arrows indicate vacuoles. (For interpretation of the references to color in this figure legend, the reader is referred to the Web version of this article.)

Author contributions

Author contributions Conceptualization: Claudia Pessoa; Formal analysis and investigation: Luciana V. Rebouças, Fátima C. E. Oliveira, and Daniel P. Pinheiro; Methodology: Fátima C. E. Oliveira, Augusto C. A. Oliveira, Renata G. Almeida, Eufrânio N. da Silva Júnior, Marcia S. Rizzo, Marcília P. Costa, Guilherme Zocolo, Fábio O. S. Ribeiro, Durcilene A. da Silva, Maria F. S. Silva, Vanessa P. G. Ferreira and Roberto Nicolete; Writing – original draft preparation: Luciana V. Rebouças; Writing – review and editing: Daniel P. Pinheiro, Eufrânio N. da Silva Júnior, Marcília P. Costa, Guilherme Zocolo, Vanessa P. G. Ferreira and Roberto Nicolete; Resources: Claudia Pessoa, Eufrânio N. da Silva Júnior, Guilherme Zocolo, Durcilene A. da Silva and Claudia Pessoa; Supervision: Claudia Pessoa.

Declaration of competing interest

The authors declare that they have no conflict of interest.

Acknowledgments

We thank the National Cancer Institute (Bethesda, MD, USA) for the donation of tumor cell lines used in this study and thank the Brazilian Agricultural Research Corporation, called EMBRAPA (Fortaleza, CE,

Brazil), for collaboration in necessary analytical measurements.

Appendix A. Supplementary data

Supplementary data to this article can be found online at https://doi.org/10.1016/j.jddst.2021.102348.

Funding information

The authors are grateful to the Brazilian National Council of Scientific and Technological Development (Conselho Nacional de Desenvolvimento Científico e Tecnológico-CNPq) for the financial support granted to C. Pessoa (PQ-1B, Process nº: 303,102/2013-6).

References

[1] D. Hanahan, R.A. Weinberg, Hallmarks of cancer: the next generation, Cell 144 (2011) 646–674, https://doi.org/10.1016/j.cell.2011.02.013.
[2] World Health Organization (WHO), Cancer fact sheets. https://gco.iarc.fr/today/data/factsheets/cancers/39-All-cancers-fact-sheet.pdf, 2020. (Accessed 29 April 2020).
[3] A. Jemal, L. Torre, I. Soerjomataram, F. Bray, The Cancer Atlas, American Cancer Society, Atlanta, 2019.
[4] World Health Organization (WHO), Key statistics. https://www.who.int/cancer/resources/keyfacts/en/, 2020. (Accessed 29 April 2020).
[5] H. Maeda, M. Khatami, Analyses of repeated failures in cancer therapy for solid tumors: poor tumor-selective drug delivery, low therapeutic efficacy and unsustainable costs, Clin. Transl. Med. 7 (11) (2018) 1–20, https://doi.org/10.1186/s40169-018-0185-6.
[6] A.L. Lourenço, P.A. Abreu, B. Leal, E.N. da Silva Júnior, A.V. Pinto, M.C. Pinto, A. M. Souza, J.S. Novais, M.B. Paiva, L.M. Cabral, C.R. Rodrigues, V.F. Ferreira, H. C. Castro, Identification of nor-beta-lapachone derivatives as potential antibacterial compounds against *Enterococcus faecalis* clinical strain, Curr. Microbiol. 62 (v) (2011) 684–689, https://doi.org/10.1007/s00284-010-9763-6.
[7] C.N. Pinto, A.P. Dantas, K.C. de Moura, F.S. Emery, P.F. Polequevitch, M.C. Pinto, S.L. de Castro, A.V. Pinto, Chemical reactivity studies with naphthoquinones from Tabebuia with anti-trypanosomal efficacy, Arzneim Forsch/Drug Res. 50 (12) (2000) 1120–1128, https://doi.org/10.1055/s-0031-1300337.
[8] T.P. Barbosa, C.A. Camara, T.M.S. Silva, R.M. Martins, A.C. Pinto, M.D. Vargas, New 1,2,3,4-tetrahydro-1-aza-anthraquinones and 2-aminoalkyl compounds from norlapachol with molluscicidal activity, Bioorg. Med. Chem. 13 (23) (2005) 6464–6469, https://doi.org/10.1016/j.bmc.2005.06.068.
[9] E.R. Almeida, A.A. da Silva-Filho, E.R. dos Santos, C.A. Lopes, Antiinflammatory action of lapachol, J. Ethnopharmacol. 29 (2) (1990) 239–241.
[10] M.M. Sitônio, C.H. Carvalho-Júnior, A. Campos-Ide, J.B. Silva, M.C. Lima, A. J. Góes, M.B. Maia, P.J. Rolim-Neto, T.G. Silva, Anti-inflammatory and anti-arthritic activities of 3,4-dihydro-2,2-dimethyl-2H-naphthol[1,2-b]pyran-5,6-dione (β-lapachone), Inflamm. Res. 62 (1) (2013) 107–113, https://doi.org/10.1007/s00011-012-0557-0.
[11] T.T. Guimarães, M.C.F.R. Pinto, J.S. Lanza, M.N. Melo, R.L. Monte-Neto, I.M. M. Melo, E.B.T. Diogo, V.F. Ferreira, C.A. Camara, W.O. Valença, R.N. Oliveira, F. Frézard, E.N. Silva-Júnior, Potent naphthoquinones against antimony-sensitive and -resistant Leishmania parasites: synthesis of novel α- and nor-α-lapachone-based 1,2,3-triazoles by copper-catalyzed azide–alkyne cycloaddition, Eur. J. Med. Chem. 63 (2013) 523–530, https://doi.org/10.1016/j.ejmech.2013.02.038.
[12] S.L.S. Gomes, G.C.G. Militão, A.M. Costa, C. Ó Pessoa, L.V. Costa-Lotufo, E. F. Cunha-Junior, E.C. Torres-Santos, P.R.R. Costa, A.J.M. Silva, Suzuki-miyaura coupling between 3-Iodolawsone and arylboronic acids. Synthesis of lapachol analogues with antineoplastic and antileishmanial activities, J. Braz. Chem. Soc. 28 (8) (2017) 1573–1584, https://doi.org/10.21577/0103-5053.20160326.
[13] T.M. Ngoc, N.T.T. Phuong, N.M. Khoi, S. Park, H.J. Kwak, N.X. Nhiem, B.T. T. Trang, B.H. Tai, J.H. Song, H.J. Ko, S.H. Kim, A new naphthoquinone analogue and antiviral constituents from the root of *Rhinacanthus nasutus*, Nat. Prod. Res. 33 (3) (2019) 360–366, https://doi.org/10.1080/14786419.2018.1452004.
[14] M.A. Strauch, M.A. Tomaz, M. Monteiro-Machado, B.L. Cons, F.C. Patrão-Neto, J. M. Teixeira-Cruz, M.S. Tavares-Henriques, P.D. Nogueira-Souza, S.L.S. Gomes, P.R. R. Costa, E. Schaeffer, A.J.M. Silva, P.A. Melo, Lapachol and synthetic derivatives: *in vitro* and *in vivo* activities against Bothrops snake venoms, PloS One 14 (1) (2019) 1–18, https://doi.org/10.1371/journal.pone.0211229.
[15] V.C. Roa-Linares, Y. Miranda-Brand, V. Tangarife-Castaño, R. Ochoa, P.A. García, M.Á. Castro, L. Betancur-Galvis, A. San Feliciano, Anti-herpetic, anti-dengue and antineoplastic activities of simple and heterocycle-fused derivatives of terpenyl-1,4-naphthoquinone and 1,4-anthraquinone, Molecules 24 (7) (2019) 1–17, https://doi.org/10.3390/molecules24071279.
[16] E.N. da Silva Júnior, G.A.M. Jardim, C. Jacob, U. Dhawa, L. Ackermann, S.L. de Castro, Synthesis of quinones with highlighted biological applications: a critical update on the strategies towards bioactive compounds with emphasis on lapachones, Eur. J. Med. Chem. 179 (2019) 863–915, https://doi.org/10.1016/j.ejmech.2019.06.056.
[17] B.C. Cavalcanti, F.W. Barros, I.O. Cabral, J.R. Ferreira, H.I. Magalhães, H.V. Júnior, E.N. da Silva Júnior, F.C. de Abreu, C.O. Costa, M.O. Goulart, M.O. Moraes, C. Pessoa, Preclinical genotoxicology of nor-β-lapachone in human cultured lymphocytes and Chinese hamster lung fibroblasts, Chem. Res. Toxicol. 24 (9) (2011) 1560–1574, https://doi.org/10.1021/tx200180y 10.1021/tx200180y.
[18] E.N. da Silva Júnior, M.C.B. de Souza, A.V. Pinto, F.R. Maria do Carmo, M. O. Goulart, F.W. Barros, C. Pessoa, L.V. Costa-Lotufo, R.C. Montenegro, M.O. de Moraes, V.F. Ferreira, Synthesis and potent antitumor activity of new arylamino derivatives of nor-β-lapachone and nor-α-lapachone, Bioorg. Med. Chem. 15 (22) (2007) 7035–7041, https://doi.org/10.1016/j.bmc.200 7.07.043.
[19] E.N. da Silva Júnior, C.F. de Deus, B.C. Cavalcanti, C. Pessoa, L.V. Costa-Lotufo, R. Montenegro, M.O. de Moraes, M.C.F.R. Pinto, C.A. de Simone, V.F. Ferreira, M. O.F. Goulart, C.K.Z. Andrade, A.V.C. Pinto, 3-Arylamino and 3-alkoxy-nor-β-lapachone derivatives: synthesis and cytotoxicity against cancer cell lines, J. Med. Chem. 53 (1) (2010) 504–508, https://doi.org/10.1021/jm900865m.
[20] B.C. Cavalcanti, I.O. Cabral, F.A.R. Rodrigues, F.W.A. Barros, D.D. Rocha, H.I. F. Magalhães, D.J. Moura, J. Saffi, J.A.P. Henriques, T.S.C. Carvalho, M.O. Moraes, C. Pessoa, I.M.M. Melo, E.N. da Silva Júnior, Potent antileukemic action of naphthoquinoidal compounds: evidence for an intrinsic death mechanism based on oxidative stress and inhibition of DNA repair, J. Braz. Chem. Soc. 24 (1) (2013) 145–163, https://doi.org/10.1590/S0103-50532013000100019.
[21] E.H.G. Cruz, C.M.B. Hussene, G.C. Dias, E.B.T. Diogo, I.M.M. Melo, B.L. Rodrigues, M.G. Silva, W.O. Valença, C.A. Camara, R.N. Oliveira, Y.G. Paiva, M.O.F. Goulart, B.C. Cavalcanti, C. Pessoa, E.N. da Silva Junior, 1,2,3-Triazole-, arylamino- and thio-substituted1,4-naphthoquinones: potent antitumor activity, electrochemicalaspects, and bioisosteric replacement of C-ring-modified lapachones, ioorg. Med. Chem. 22 (5) (2014) 1608–1619, https://doi.org/10.1016/j.bmc.2014.01.033.
[22] J.L. Bolton, M.A. Trush, T.M. Penning, G. Dryhurst, T.J. Monks, Role of quinones in toxicology, Chem. Res. Toxicol. 13 (3) (2000) 135–160, https://doi.org/10.1021/tx9902082.
[23] J.L. Bolton, T. Dunlap, Formation and biological targets of quinones: cytotoxic versus cytoprotective effects, Chem. Res. Toxicol. 30 (1) (2017) 13–37, https://doi.org/10.1021/acs.chemrestox.6b00256.
[24] Y. Kumagai, Y. Shinkai, T. Miura, A.K. Cho, The chemical biology of naphthoquinones and its environmental implications, An. Ver. Pharmacol. Toxicol. 52 (2012) 221–247, https://doi.org/10.1146/annurev-pharmtox-010611-134517.
[25] D.P. Pinheiro, Evaluation of the Cytotoxic Potential and Molecular Mechanism of Synthetic Naphthoquinones ENSJ39 and ENSJ108: in Vitro and in Vivo Studies. Thesis (Doctoral), Federal University of Ceará, 2017. Ceará/Brazil, http://www.repositorio.ufc.br/bitstream/riufc/26907/1/2017_tese_dppinheiro.pdf. (Accessed 1 April 2020), 2020.
[26] B.C. Cavalcanti, H. Magalhães, F. Rodrigues, M.O. Moraes, C. Pessoa, Arylamino-*nor*-β-lapachone derivative-induced apoptosis in human prostate cancer cells: involvement of NAD(P)H:quinone oxidoreductase (NQO1), BMC Proc. 7 (Suppl 2) (2013) 12, https://doi.org/10.1186/1753-6561-7-S2-P12.
[27] V.S. de Sena Pereira, C.B. Silva de Oliveira, F. Fumagalli, F. da Silva Emery, N.B. da Silva, V.F. de Andrade Neto, Cytotoxicity, hemolysis and *in vivo* acute toxicity of 2-hydroxy-3-anilino-1,4-naphthoquinone derivatives, Toxicol. Rep. 3 (2016) 756–762, https://doi.org/10.1016/j.toxrep.2016.09.007.
[28] B.K. Aithal BK, M.R.S. Kumar, B.N. Rao, R. Upadhya, V. Prabhu, G. Shavi, K. Arumugam, S.P. Sajankila, N. Udupa, K. Satyamoorthy, B.S.S. Rao, Evaluation of pharmacokinetic, biodistribution, pharmacodynamic, and toxicity profile of free juglone and its sterically stabilized liposomes, J. Pharmaceut. Sci. 100 (8) (2011) 3517–3528, https://doi.org/10.1002/jps.22573.
[29] R. Munday, B.L. Smith, C.M. Munday, Comparative toxicity of 2-hydroxy-3-alkyl-1,4-naphthoquinones in rats, Chem. Biol. Interact. 98 (2) (1995) 185–192, https://doi.org/10.1016/0009-2797(95)03645-8.
[30] R. Munday, B.L. Smith, C.M. Munday, Effect of inducers of DT-diaphorase on the haemolyticactivity and nephrotoxicity of 2-amino-1,4-naphthoquinone in rats, Chem. Biol. Interact. 155 (3) (2005) 140–147, https://doi.org/10.1016/j.cbi.2005.06.001.
[31] R. Munday, B.L. Smith, C.M. Munday, Structure-activity relationships in the haemolytic activityand nephrotoxicity of derivatives of 1,2- and 1,4-naphthoquinone, J. Appl. Toxicol. 27 (3) (2007) 262–269, https://doi.org/10.1002/jat.1206.
[32] R.Y. Yang, D. Kizer, H. Wu, E. Volckova, X.S. Miao, S.M. Ali, M. Tandon, R. E. Savage, T.C. Chan, M.A. Ashwell, Synthetic methods for the preparation of ARQ 501 (*β*–lapachone) humam blood metabolites, Bioorg. Med. Chem. 16 (10) (2008) 5635–5643, https://doi.org/10.1016/j.bmc.2008.03.073.
[33] F.C. de Abreu, D.C.M. Ferreira, M.O.F. Goulart, O. Buriez, C. Amarote, Electrochemical activation of β-lapachone in β-cyclodextrin inclusion complexes and reactivity of its reduced form towards oxygen in aqueous solutinons, J. Electroanal. Chem. 608 (2) (2007) 125–132, https://doi.org/10.1016/j.jelechem.20 07.05.020.
[34] K.H. Kim, T. Le, H.K. Oh, B. Heo, J. Moon, S. Shin, S.H. Jeong, Protective microencapsulation of β-lapachone using porous glass membrane technique based on experimental optimisation, J. Microencapsul. 34 (6) (2017) 545–559, https://doi.org/10.1080/02652048.2017.1367850.
[35] M.P. Costa, A.C.S. Feitosa, F.C.E. Oliveira, B.C. Cavalcanti, G.C. Dias, E.W. S. Caetano, F.A.M. Sales, V.N. Freire, S.D. Fiore, R. Fischer, L.O. Ladeira, E.N. da Silva Júnior, C. Pessoa, Encapsulation of nor-β-lapachone into poly(D,L)-lactide-co-glycolide (PLGA) microcapsules: full characterization, computational details and cytotoxic activity against human cancer cell lines, Med. Chem. Commun. 8 (10) (2017) 1993–2002, https://doi.org/10.1039/C4MD00371C.
[36] M.P. Costa, A.C. Feitosa, F.C. Oliveira, B.C. Cavalcanti, E.M. da Silva, G.G. Dias, F. A. Sales, B.L. Sousa, I.L. Barroso-Neto, C. Pessoa, E.W. Caetano, S. Di Fiore, R. Fischer, L.O. Ladeira, V.N. Freire, Controlled release of nor-β-lapachone by plga

microparticles: a strategy for improving cytotoxicity against prostate cancer cells, Molecules 21 (7) (2016) 873, https://doi.org/10.3390/molecules21070873.
[37] T. Arasoglu, B. Mansuroglu, S. Derman, B. Gumus, B. Kocyigit, T. Acar, I. Kocacaliskan, Enhancement of antifungal activity of juglone (5-hydroxy-1,4-naphthoquinone) using a poly(d,l-lactic-co-glycolic acid) (PLGA) nanoparticle system, J. Agric. Food Chem. 64 (38) (2016) 7087–7094, https://doi.org/10.1021/acs.jafc.6b03309.
[38] I.M. Cavalcanti, E.A. Mendonça, M.C. Lira, S.B. Honrato, C.A. Camara, R. V. Amorim, J. Mendes-Filho, M.M. Rabello, M.Z. Hernandes, A.P. Ayala, N. S. Santos-Magalhães, The encapsulation of β-lapachone in 2-hydroxypropyl-β-cyclodextrin inclusion complex into liposomes: a physicochemical evaluation and molecular modeling approach, Eur. J. Pharmaceut. Sci. 44 (3) (2011) 332–340, https://doi.org/10.1016/j.ejps.2011.08.011.
[39] F. Farjadian, A. Ghasemi, O. Gohari, A. Roointan, M. Karimi, M.R. Hamblin, Nanopharmaceuticals and nanomedicines currently on the market: challenges and opportunities, Nanomedicine 14 (1) (2019) 93–126, https://doi.org/10.2217/nnm-2018-0120.
[40] J. Hare, T. Lammers, M.B. Ashford, S. Puri, G. Storm, S.T. Barry, Challenges and strategies in anti-cancer nanomedicine development: an industry perspective, Adv. Drug Deliv. Rev. 108 (2017) 25–38, https://doi.org/10.1016/j.addr.2016.04.025.
[41] J.O. Eloy, R. Petrilli, F.S.G. Praça, M. Chorillic, Recent advances with targeted liposomes for drug delivery, in: V. Torchilin (Ed.), Handbook of Materials for Nanomedicine: Lipid-Based and Inorganic Nanomaterials, Jenny Stanford Publishing, New York, 2020, pp. 85–122.
[42] Y. Panahi, M. Farshbaf, M. Mohammadhosseini, M. Mirahadi, R. Khalilov, S. Saghfi, A. Akbarzadeh, Recent advances on liposomal nanoparticles: synthesis, characterization and biomedical applications. Artif Cells Nanomed, Biotechnol. 45 (4) (2017) 788–799, https://doi.org/10.1080/21691401.2017.1282496.
[43] J. Kalra, M.B. Bally, Lipossomes, in: W.P. Cheng, A. Lalatsa (Eds.), Uchegbu IF, Schätzlein AG, Springer Fundamentals of Pharmaceutical Nanoscience, Springer Science, New York, 2013, pp. 27–63.
[44] G. Bozzuto, A. Molinari, Liposomes as nanomedical devices, Int. J. Nanomed. 10 (2015) 975–999, https://doi.org/10.2147/IJN.S68861.
[45] D. Lasic, Liposomes, Am. Sci. 80 (1) (1992) 20–31. www.jstor.org/stable/29774555.
[46] F.M. Sombra, A.R. Richter, A.R. de Araújo, F.O.S. Ribeiro, J.F.S. Mendes, R.O. S. Fontenelle, D.A. da Silva, A.C.B. de Paula, J.P.A. Feitosa, F.M. Goycoolea, R.C. M. de Paula, Nanocapsules of *Sterculia striata* acetylated polysaccharide as a potential monomeric amphotericin B delivery matrix, Int. J. Biol. Macromol. 130 (1) (2019) 655–663, https://doi.org/10.1016/j.ijbiomac.2019.02.076.
[47] T. Mosmann, Rapid colorimetric assay for cellular growth and survival: application to proliferation and cytotoxicity assays, J. Immunol. Methods 65 (1) (1983) 55–63, https://doi.org/10.1016/0022-1759(83)90303-4.
[48] W. Strober, Trypan blue exclusion test of cell viability, Curr. Protoc. Im. 111 (1) (2015) A3B1–A3B3, https://doi.org/10.1002/0471142735.ima03bs111.
[49] Official Journal of the European Union, Commission recommendation of 18 October 2011 on the definition of nanomaterial (2011/696/EU), 2019 November 08. Available from: https://ec.europa.eu/research/industrial_technologies/pdf/policy/commission-recommendation-on-the-definition-of-nanomater18102011_en.pdf.
[50] V.R. Patel, Y.K. Agrawal, Nanosuspension: an approach to enhance solubility of drugs, "J. Adv. Pharm. Technol. Research"" (JAPTR)" 2 (2) (2011) 81–87, https://doi.org/10.4103/2231-4040.82950.
[51] H. Chen, X. Chang, D. Du, W. Liu, J. Liu, T. Weng, Y. Yang, Y. Xu, X. Yang, Podophyllotoxin-loaded solid lipid nanoparticles for epidermal targeting, J. Contr. Release 110 (2) (2006) 296–306, https://doi.org/10.1016/j.jconrel.2005.09.052.
[52] S. Bhattacharjee, DLS and zeta potential – what they are and what they are not? J. Contr. Release 235 (2016) 337–351, https://doi.org/10.1016/j.jconrel.2016.06.017.
[53] C.M. Batista, C.M.B. Carvalho, N.S.S. Magalhães, Liposomes and their therapeutic: state of art applications, Rev. Bras. Ciencias Farm. 43 (2) (2007) 167–179, https://doi.org/10.1590/S1516-93322007000200003.
[54] Y. Chen, J. Chen, Y. Cheng, L. Luo, P. Zheng, Y. Tong, Z. Li, A lyophilized sterically stabilized liposome-containing docetaxel: *in vitro* and *in vivo* evaluation, J. Liposome Res. 27 (1) (2017) 64–73, https://doi.org/10.3109/08982104.2016.1158185.
[55] N. Changsan, H. Chan, F. Separovic, T. Srichana, Physicochemical characterization and stability of rifampicin liposome dry powder formulations for Inhalation, J. Pharmaceut. Sci. 98 (2) (2009) 628–639, https://doi.org/10.1002/jps.21441.
[56] A. Akbarzadeh, R. Rezaei-Sadabady, S. Davaran, S.W. Joo, N. Zarghami, Y. Hanifehpour, M. Samiei, M. Kouhi, L. Nejati-Koshki, Liposome: classification, preparation, and applications, Nanoscale Res. Lett. 8 (102) (2013) 1–9, https://doi.org/10.1186/1556-276X-8-102.
[57] M.C.B. Lira, M.P. Siqueira-Moura, H.M.L. Rolim-Santos, F.C.S. Galetti, A. R. Simioni, N.P. Santos, E.S.T. do Egito, S.L. Silva, A.C. Tedesco, N.S. Santos-Magalhães, *In vitro* uptake and antimycobacterial activity of liposomal usnic acid formulation, J. Liposome Res. 19 (1) (2009) 49–58, https://doi.org/10.1080/08982100802564628.
[58] I. Onyesom, D.A. Lamprou, L. Sygellou, S.K. Owusu-Ware, M. Antonijevic, B. Z. Chowdhry, D. Douroumis, Sirolimus encapsulated liposomes for cancer therapy: physicochemical and mechanical characterization of sirolimus distribution within liposome bilayers, Mol. Pharm. 10 (11) (2013) 4281–4293, https://doi.org/10.1021/mp400362v.
[59] V. Nekkanti, S. Kalepu, Recent advances in liposomal drug delivery: a review, Pharm. Nanotechnol. 3 (1) (2015) 35–55, https://doi.org/10.2174/2211738503666150709173905.
[60] C. Demetzos, Differential scanning calorimetry (DSC): a tool to study the thermal behavior of lipid bilayers and liposomal stability, J. Liposome Res. 18 (3) (2008) 159–173, https://doi.org/10.1080/08982100802310261.
[61] J.O. Eloy, R. Petrilli, J.F. Topan, H. Antonio, J. Barcellos, D.L. Chesca, L.N. Serafini, D.G. Tiezzi, R.J. Lee, J.M. Marchetti, Co-loaded paclitaxel/rapamycin liposomes: development, characterization and in vitro and in vivo evaluation for breast cancer therapy, Colloids Surf. B Biointerfaces 141 (2016) 74–82, https://doi.org/10.1016/j.colsurfb.2016.01.032.
[62] V. Sanna, A.M. Roggio, S. Siliani, M. Piccinini, S. Marceddu, A. Mariani, M. Sechi, Development of novel cationic chitosan-and anionic alginate-coated poly (d, l-lactideco-glycolide) nanoparticles for controlled release and light protection of resveratrol, Int. J. Nanomed. 7 (2012) 5501–5516, https://doi.org/10.2147/IJN.S36684.
[63] A.S. Zidan, O.A. Sammour, M.A. Hammad, N.A. Megrab, M.D. Hussain, M. Khan, M.J. Habib, Formulation of anastrozole microparticles as biodegradable anticancer drug carriers, AAPS PharmSciTech 7 (2006) E1–E9, https://doi.org/10.1208/pt070361.
[64] J.O. Eloy, J. Saraiva, S. de Albuquerque, J.M.M. Marchetti, Solid dispersion of ursolic acid in gelucire 50/13: a strategy to enhance drug release and trypanocidal activity, AAPS PharmSciTech 13 (2012) 1436–1445, https://doi.org/10.1208/s12249-012-9868-2.
[65] L.C. Gayoso, A.I. Morenoa, H.M.L. Rolima, R.M. Freitasa, N.S. Santos-Magalhães, Antidepressant-like activity of liposomal formulation containingnimodipine treatment in the tail suspension test, forced swim test and MAOB activity in mice, Brain Res. J. 1646 (1) (2016) 235–240, https://doi.org/10.1016/j.brainres.2016.06.004 10.1016/j.brainres.2016.06.004.
[66] I.M.F. Cavalcanti, T.G.C. Menezes, L.A.A. Campos, M.S.F. Ferraz, M.A.V. Maciel, M. N.P. Caetano, N.S. Santos-Magalhães, Interaction study between vancomycin and liposomes containing natural compounds against methicillin-resistant *Staphylococcus aureus* clinical isolates, Braz. J. Pharm. Sci. 54 (2) (2018) 1–8, https://doi.org/10.1590/s2175-97902018000200203.
[67] E. Blanco, E.A. Bey, Y. Dong, B.D. Weinberg, D.M. Sutton, D.A. Boothman, J. Gao, β-Lapachone-containing PEG–PLA polymer micelles as novel nanotherapeutics against NQO1-overexpressing tumor cells, J. Contr. Release 122 (3) (2007) 365–374, https://doi.org/10.1016/j.jconrel.2007.04.014.
[68] R.I. Bello, C. Gómez-Díaz, G. López-Lluch, N. Forthoffer, M.C. Córdoba-Pedregosa, P. Navas, J.M. Villalba, Dicoumarol relieves serum withdrawal-induced G0/1 blockade in HL-60 cells through a superoxide-dependent mechanism, Biochem. Pharmacol. 69 (11) (2005) 1613–1625, https://doi.org/10.1016/j.bcp.2005.03.012.
[69] J. Fourie, C.J. Oleschuk, F.J. Guziec, L. Guziec, D.J. Fiterman, C. Monterrosa, A. Begleiter, The effect of functional groups on reduction and activation of quinone bioreductive agents by DT-diaphorase, Canc. Chemother. Pharmacol. 49 (2002) 101–110, https://doi.org/10.1007/s00280-001-0395-1.
[70] E.A. Bey, M.S. Bentle, K.E. Reinicke, Y. Dong, C.R. Yang, L. Girard, J.D. Minna, W. G. Bornmann, J. Gao, D.A. Boothman, An NQO1- and PARP-1-mediated cell death pathway induced in non-small-cell lung cancer cells by beta-lapachone, Proc. Natl. Acad. Sci. U.S.A. 104 (28) (2007) 11832–11837, https://doi.org/10.1073/pnas.0702176104.
[71] M. Ough, A. Lewis, E.A. Bey, J. Gao, J.M. Ritchie, W. Bornmann, D.A. Boothman, L. W. Oberley, J.J. Cullen, Efficacy of beta-lapachone in pancreatic cancer treatment: exploiting the novel, therapeutic target NQO1, Canc. Biol. Ther. 4 (1) (2005) 95–102, https://doi.org/10.4161/cbt.4.1.1382. https://doi.org/10.4161/cbt.4.1.1382.
[72] E. Pérez-Sacau, R.G. Díaz-Peñate, A. Estévez-Braun, A.G. Ravelo, J.M. García-Castellano, L. Pardo, M. Campillo, Synthesis and pharmacophore modeling of naphthoquinone derivatives with cytotoxic activity in human promyelocytic leukemia HL-60 cell line, J. Med. Chem. 50 (4) (2007) 696–706, https://doi.org/10.1021/jm060849b.
[73] S.H. Jung, S.H. Jung, H. Seong, S.H. Cho, K.S. Jeong, B.C. Shin, Polyethylene glycol-complexed cationic liposomes for enhanced cellular uptake and anticancer activity, Int. J. Pharm. 382 (1) (2009) 254–261, https://doi.org/10.1016/j.ijpharm.2009.08.002.
[74] J. Wu, A. Lee, Y. Lu, R.J. Lee, Vascular targeting of doxorubicin using cationic liposomes, Int. J. Pharm. 337 (1) (2007) 329–335, https://doi.org/10.1016/j.ijpharm.2007.01.003.
[75] P. Deol, G.K. Khuller, Lung specific stealth liposomes: stability, biodistribution, and toxicity of liposomal antitubercular drugs in mice, Biochim. Biophys. Acta 1334 (2) (1997) 161–172, https://doi.org/10.1016/s0304-4165(96)00088-8.
[76] D.C. Drummond, C.O. Noble, M.E. Hayes, J.W. Park, D.B. Kirpotin, Pharmacokinetics and *in vivo* drug release rates in liposomal nanocarrier development, J. Pharmaceut. Sci. 97 (11) (2008) 4696–4740, https://doi.org/10.1002/jps.21358.
[77] J.A. Kamps, Assessment of liposome–cell interactions, Methods Mol. Biol. 606 (2010) 199–207, https://doi.org/10.1007/978-1-60761-447-0_15.